



European Geosciences Union General Assembly 2015, EGU

Division Energy, Resources & the Environment, ERE

## Matching pressure measurements and observed CO<sub>2</sub> arrival times with static and dynamic modelling at the Ketzin storage site

Holger Class<sup>a,\*</sup>, Lena Mahl<sup>a</sup>, Waqas Ahmed<sup>a</sup>, Ben Norden<sup>b</sup>, Michael Kühn<sup>b</sup>,  
Thomas Kempka<sup>b</sup>

<sup>a</sup>*Institute for Modelling Hydraulic and Environmental Systems, Universität Stuttgart, Pfaffenwaldring 61, 70569 Stuttgart, Germany*

<sup>b</sup>*GFZ German Research Centre for Geosciences, Telegrafenberg, 14473 Potsdam, Germany*

### Abstract

At the Ketzin pilot site 67,000 tonnes of CO<sub>2</sub> were injected between 2008 and 2013 into a sandstone formation. Pressure monitoring and observation of CO<sub>2</sub> arrival in two observation wells provide valuable field measurements for history matching. Modelling of the CO<sub>2</sub> injection faces several challenges and uncertainties as discussed in this study. Different approaches towards matching the observed data are presented. It can be shown that a calibration of the simulation models (ECLIPSE E100 and Dumux) to the data is possible with good accuracy, while considerable uncertainties in the model parameters remain, to a large amount resulting from strong correlations between permeability and porosity.

© 2015 The Authors. Published by Elsevier Ltd. This is an open access article under the CC BY-NC-ND license (<http://creativecommons.org/licenses/by-nc-nd/4.0/>).

Peer-review under responsibility of the GFZ German Research Centre for Geosciences

**Keywords:** CO<sub>2</sub> storage, numerical modeling, history matching, Ketzin pilot site

### 1. Introduction

The Ketzin pilot site in Brandenburg/Germany was the first on-shore CO<sub>2</sub> storage site in Europe and the only active one in Germany. The depth of the used saline aquifer is at about 630 m to 650 m near the injector [1]. CO<sub>2</sub> storage in Ketzin started in June 2008 and was regularly stopped in August 2013. A total amount of about 67,000 tonnes of CO<sub>2</sub> was injected at slightly supercritical pressure and temperature into the 74 m thick Stuttgart Formation. The lithology of the formation is heterogeneous, composed of sand channels of high permeability embedded in flood plain facies rocks with low permeability [2]. Three wells were drilled before the injection: The Ktzi 201 as injection and observation well and Ktzi 201 and Ktzi 202 as observation wells. Data sets of the geological structure, seismic surveys [3], core material information and well-log data [4], and hydraulic pumping tests [5] are available.

\* Corresponding author. Tel.: +49-711-685-64678 ; Fax: +49-711-685-60430.  
E-mail address: [holger.class@iws.uni-stuttgart.de](mailto:holger.class@iws.uni-stuttgart.de)

The primary task of numerical modelling work for Ketzin since the project start in 2004 has been the development of calibrated and - to some extent - predictive models. The available data include continuous pressure monitoring at the Ktzi 201 injection well and, for about one year, also at the Ktzi 202 borehole as well as the arrival times of the CO<sub>2</sub> at the two observation wells. Varying injection rates lead to a corresponding pressure response in the reservoir. A matching of measurement and simulations would give a reliable estimate of the order of magnitude of the reservoir permeability. In fact, a match of the observed pressure after injection is considered the most important prerequisite for predictive assessments in the reservoir. The observed early CO<sub>2</sub> arrival at the first observation well (21.7 days) provides information only for the immediate vicinity of the injection well (50 m). We discuss the implications on the reliability of estimated parameters from a successful pressure match in comparison to a match of the arrival times.

History matching is common practice in reservoir engineering, e.g. [6], often applied as an iterative trial-and-error process by adjusting the geological model to reproduce observations like oil or gas production rates and pressure responses, see e.g. [7]. Other approaches rely on sophisticated statistics with a focus on probability estimates to exclude less probable realizations of the geological model, e.g. [8]. This study has its focus on the Ketzin CO<sub>2</sub> storage project as a showcase with best-possible site exploration and monitoring over several years. We follow the traditional trial-and-error approach, while also including inverse modelling techniques for some parameter estimates. The history matching is performed with two different numerical simulators: the industry standard code ECLIPSE [9] and the scientific dynamic flow model Dumux [10]. Using Dumux, we tested different approaches to match the data available in late 2012, while trying to identify the most sensitive parameters and to reduce the arbitrariness of decisions for fitting model parameters to data. Since the approaches for the history matching were chosen almost independently by the different modelers, this study can be viewed also as an intercomparison study. For example, previous benchmark studies on CO<sub>2</sub> storage related problems revealed that the influence of different codes on the simulation results is much smaller than the influence of the decisions and choices made by the modelers [11], and that geology is the most important factor of uncertainty in actual projects.

## 2. Remarks on the static geological model and the applied simulators ECLIPSE 100 and Dumux

Details on lithology and mineralogy, the depositional system, available data, and the set-up of the primary geological model are presented by Förster et al. [12] and Norden & Frykman [13]. Based on additional monitoring data, the geological model was updated and modified as reported in Kempka et al. [14], which is the basis for the present study. The reservoir model follows an integrated geological concept considering the basin-wide observed characteristics of the formation and site-specific point and spatial data. The geological model was subdivided into three zones with different discretization. The uppermost zone with a thickness of 24 m is discretized by 0.5 m in the vertical, while 1 m steps were used for the 12 m interval below and the 36 m thick lowermost zone with 3 m steps. For all zones, the horizontal resolution of the geological model is 5 m × 5 m and the conceptual facies model considers two major types, a floodplain and a sand channel facies. The distribution of petrophysical properties within the facies was modeled using a sequential Gaussian simulation with the Petrel software package, mainly based on the petrophysical core and log data available from the site [4]. From spectral decomposition of the 3D seismic data and trend-maps of total porosity were calculated, allowing a co-Kriging of this parameter for the channel facies. Then, effective porosity was modeled based on established variograms and using a co-Kriging algorithm considering the results of the total porosity simulation. In a last step, permeability was calculated using the determined poro-perm relationship for the different facies environment [13].

The software package *ECLIPSE 100* [9] is a black-oil simulator using the finite-difference method for spatial discretization. It can handle up to four phases (gas, oil, water, and a tracer) under isothermal conditions. In order to allow for simulation of CO<sub>2</sub> solubility in brine, the ECLIPSE 100 oil and gas phases were adapted to represent the brine and CO<sub>2</sub> phases, respectively. *Dumux* [10] is an open-source software under the GPL license for simulating flow and transport in porous media, including compositional, non-isothermal, multi-scale or multi-physics approaches. *Dumux* is based on DUNE [15], which features slim interfaces for an efficient use of inheritance and new libraries. We used here a subdomain collocation method (BOX), i.e. a dual mesh approach with finite-volume properties, where gradients of pressure, mass fraction, etc., are approximated by finite-element shape functions. The BOX method was applied for an unstructured tetrahedron mesh, while a cell-centered finite-volume method was applied for a hexahedron mesh in a previous study. Both ECLIPSE 100 and Dumux solve the equations fully implicit in time.

### 3. Approaches towards history matching

Correlations between model parameters impede the finding of a unique set of parameters by a calibration, the more so where the real geology is (a) not exactly known and (b) the available geological model is mapped to even coarser meshes for simulating the far-field flow and transport processes. More degrees of freedom, i.e. a larger number of estimated parameters, increase the chance of obtaining a good history match. But the more calibration parameters, the more correlations occur, reducing the uniqueness of the obtained set of best-fit parameters. The approaches introduced below differ in the set of calibration parameters and in the applied concepts to find the sets of best-fit parameters. Meshes were constructed with particular focus on fine spatial resolution in the vicinity of the wells, i.e. in the two-phase flow region. However, in the far-well regions, the applied meshes in the dynamic simulations were coarser than the spatial resolution of the geological model. Thus, permeability and porosity had to be mapped from the hexahedral grid based geological model onto the different meshes. Dependent on the interpolation method, this results in a more or less strong deviation of the implemented geology in the dynamic flow simulations.

A few remarks are helpful on the observation data in Ketzin. The arrival times at the observation wells need to be considered with care due to the individual completion of each well which is beyond the scope to be explained here, [16]. The arrival of CO<sub>2</sub> at the wells was measured with gas membrane sensors (GMS), which were installed at a depth of 150 m below ground surface [17]. It is fair to assume that CO<sub>2</sub> reaching the observation wells will enter the open annulus in the well first, accumulate there, cross the filter screens and only then move upward within the well. Therefore, the arrival time measured by the GMS does not necessarily provide an accurate value for the CO<sub>2</sub> arrival at the well, which must be earlier than the detection by the sensor in the field. The postulated arrival times [18,19] are associated with an uncertainty of several days, indicating only that CO<sub>2</sub> has finally reached the sensors after a certain time period. Therefore, a weight-shift in the calibration process towards pressure matching is given.

#### 3.1. Approach I: Calibration with six permeability multipliers using ECLIPSE

In Approach I, we considered the manual adaptation of two permeability tensors for the entire model, i.e. a total of six permeability modifiers. As discussed by Kempka & Kühn [20], one of both permeability tensors was applied for the near-well area determined by the average simulated spatial migration of gaseous CO<sub>2</sub> after 400 days of injection, and the other one for the far-well area. Model parameterization was carried out as discussed by Kempka et al. [20,21], whereas CO<sub>2</sub> phase density and viscosity were derived here from Span & Wagner [22] instead of Peneloux et al. [23]. This required an adaptation of the six permeability modifiers in the entire model to achieve a comparable match quality to that documented by [20]. Thereto, fitting of the simulated Ktzi 201 downhole pressure was carried out by matching the near-well permeability multipliers to the observed data, while maintaining the far-well permeability multiplier at the same value. Thereafter, only the far-well multiplier was adapted to match the Ktzi 201 downhole pressure development for 1286 days of CO<sub>2</sub> injection (24/06/2008 to 31/12/2011). In a last step, both permeability tensors were fitted at the same time to achieve the final match of simulated to observed Ktzi 201 downhole pressure. Subsequently, a predictive simulation run was carried out without changing the adapted permeability multipliers for the next 908 days of injection operation (26 May 2014, 2193 days after start of injection).

#### 3.2. Approach II: Calibration using a reduced number of fitted parameters

Approach II aims at (i) reducing the number of fitted parameters and (ii) accounting for the different value of information from pressure measurements and observed CO<sub>2</sub> arrival. The pressure response of the reservoir to varying injection rates allows for an integral interpretation of hydraulic properties as permeability, porosity, and relative permeability, while the observed arrival of CO<sub>2</sub> at a well is only a point information, affected by the near-borehole geology, its individual completion and the measurement method. Thus, we put less emphasis on the CO<sub>2</sub> arrival times at the observation wells. We simply introduce a local geological barrier-like feature (see Fig. 4) for matching the arrival time at the Ktzi 202 borehole. The more degrees of freedom are chosen, the better matches the calibrated model, but increasing the number of parameters results in increased parameter correlation. Finsterle [24] stated that an overparameterisation results in higher parameter uncertainty and the effectiveness of the calibrated model is reduced.

The observed pressures and CO<sub>2</sub> arrivals at the boreholes are affected by various parameters: *Permeability* is determined by the geological model, whereby pressure evolution depends strongly on permeability. The arrival times are



Fig. 1. Tetrahedron (left) and hexahedron mesh (right) with interpolated permeability fields (five times vertically exaggerated).

also directly affected, since lower permeability retards the CO<sub>2</sub> flow. Obviously, the variation of *porosity* influences the arrival times and pressure is indirectly influenced by the pore space compressibility. Measurements of *relative permeability* are rather uncertain (see below). Since pressure and arrival times are sensitive to intrinsic permeability, they are sensitive to relative permeability as well. *Capillary pressure* measurements are also associated with uncertainties; capillary pressure is not scaled here with poro-perm data, since a scaling with the Leverett-J function had very minor influence (not shown in this study). Thus, the capillary pressure is expected to have a smaller influence on the CO<sub>2</sub> distribution in the subsurface. The *skin factor* at the injection well simulates formation damage due to drilling, which effectively can change the permeability and, thus, influence the pressure directly at the injection. For the arrival times, the influence of a skin factor is expected to be small [20,21]. The variation of *anisotropy* presented in Approach I ([20]) showed that the plume propagation is highly influenced by the anisotropy in the lateral directions; thus, the arrival time is sensitive to the anisotropy ratio. The pressure field is further influenced by the vertical direction.

The Dumux simulations use a similar setup as those with Eclipse, i.e. the geological model as explained in Sec. 2 (Fig. 1). Hydrostatic conditions with a pressure gradient as in Tab. 1 are assigned as initial and lateral boundary conditions. The model top and bottom represent no-flow boundaries. The temperature is 34 °C at 639.5 m depth with a thermal gradient of 0.03 °C/m. The parameters for salinity, anisotropy, and pore compressibility are shown in Tab. 1. A Brooks-Corey relation is used for capillary pressure based on (unpublished) data from the CO<sub>2</sub>SINK project:

$$k_{rw} = k_{rw,eq} \left( \frac{S_w - S_{wr}}{1 - S_{wr}} \right)^{n_w} \quad \text{and} \quad k_{rm} = k_{rm,eq} \left( \frac{1 - S_w - S_{nr}}{1 - S_{nr} - S_{wr}} \right)^{n_{CO_2}} \quad (1)$$

Table 1. Dumux model setup: Input parameters.

Salinity	$S=0.2 \text{ kg}_{salt}/\text{kg}_{brine}$	Brooks-Corey parameter (cap. press.)	$\lambda = 1.011613$
Pore compressibility	$C=7.2 \cdot 10^{-10} \text{ 1/Pa}$	Brooks-Corey entry pressure	$p_d = 10952.87 \text{ Pa}$
Anisotropy	$K_v/K_h=1/3$	Residual brine saturation	$S_{wr} = 0.15$
Init. pressure at 639.5 m	$p_{init}=62 \text{ bar}$	Residual CO <sub>2</sub> saturation	$S_{nr} = 0.05$
Pressure gradient	$1.14 \text{ Pa/m}$	Rel. perm. parameter	$k_{rw,eq} = 1.0$
Init. temperature at 639.5 m	$T_{init} = 34\text{C}$	Rel. perm. parameter	$k_{rCO_2,eq} = 0.85$
Temperature gradient	$0.03^\circ\text{C/m}$	Rel. perm. parameters	$n_w = 5.5, n_{CO_2} = 1.25$

Different meshes were constructed for the Dumux simulations. The first approach was a tetrahedron mesh (Fig. 1 left) with a circular refinement region around the injection and observation wells. The second mesh uses hexahedrons (Fig. 1, right) with a refinement around the wells. We discuss here only results with the hexahedron mesh with cell-centered finite volumes and refer to Kempka et al. [14] for results with the tetrahedrons.

The matching procedure involves a calibration for the initial period using inverse modelling with subsequent extrapolation in time. The procedure is tailored to keep computational efforts low: (i) Calibration of only three parameters with an inverse modeling approach using iTOUGH2 [24] is applied to match the pressure at the injection well for the first 50 days. Concurrently, the arrival time at Ktzi 200 is matched as well. (ii) The calibrated model (first 50 days) is extrapolated to predict the further behavior. (iii) The second arrival time at Ktzi 202 is matched by adapting a local geological feature as the low permeable “barrier”. This idea arises from apparently good hydraulic responses between the wells Ktzi 201 and Ktzi 202 in pumping tests [5], while there is a retardation of the CO<sub>2</sub> arrival. This can be explained by a geologic feature acting as a barrier only for the lighter phase (here the CO<sub>2</sub>) at the top of the reservoir.

## 4. Results and discussion

### 4.1. Best-fit results from Approach I

The best fit for the history matching technique applied in Approach I was achieved with the permeability multipliers listed in Tab. 2. A reduction of permeability multipliers in the near-well area compared to those in Kempka et al. [20] was necessary since a deviation in CO<sub>2</sub> density of up to 5 % between the Peneloux et al. [23] and Span & Wagner [22] equations of state (EOS) was observed at the given pressure and temperature conditions in the Stuttgart Formation. Consequently, the permeability multipliers had to be adapted to achieve an acceptable fit between simulated and observed downhole pressures at the Ktzi 201 well with the Span & Wagner EOS. However, the permeability multipliers for the far-well area were not modified in the present study.

Table 2. Permeability multipliers applied in Approach I for the ECLIPSE 100 simulation model to achieve a fit between simulated and observed downhole pressures at the Ktzi 201 well.

Reservoir model region	Permeability multiplier in		
	i-direction	j-direction	k-direction
Near-well area	0.25 [22] / 0.34 [23]	0.05 [22] / 0.07 [23]	0.05 [22] / 0.07 [23]
Far-well area	0.38	0.10	0.10

Table 3. Observed and simulated arrival times of gaseous and dissolved CO<sub>2</sub> in the observation wells Ktzi 200 and Ktzi 202 calculated using the Peneloux et al. [23] and Span & Wagner [22] equations of state, modified from [20].

Observation well	Phase	Observed (days)	Simulated (days)	Simulated (days)	Deviation (%)	Deviation (%)
			ECLIPSE Span and Wagner	ECLIPSE Peneloux et al.	ECLIPSE Span and Wagner	ECLIPSE Peneloux et al.
Ktzi 200	dissolved	-	10.0	11.0	-	-
	gaseous	21.7	18.9	20.3	12.9	6.4
Ktzi 202	dissolved	-	243.0	225.0	-	-
	gaseous	271	272.0	256.0	0.4	5.5

Simulation results shown in Fig. 5 reveal that a good match of Ktzi 201 downhole pressure is achieved for the entire time of operation. Maximum deviations occur at days 20 and 60 of the injection operation with up to 2.5 bar (about 3.2 %), since the matching procedure applied aimed at an optimal adaptation of the two permeability tensors to account for the pressure development during the first 1286 days of injection operation. Note that injection rates at the Ketzin pilot site were determined by a flow meter [1,25] with relatively high uncertainties in flow-through measurements, which had to be corrected by using the fill state of the CO<sub>2</sub> storage tank [26]. Thus, already small deviations in the corrected injection rate may result in significant pressure differences in the first weeks of operation, whereby about 1,700 tonnes of CO<sub>2</sub> were in the storage formation after 60 days of injection. The difference between simulated and observed downhole pressure in the Ktzi 201 well decreases thereafter until reaching the end of the history matching phase at 1286 days. Deviations between simulated and observed reservoir pressures stay below 1 % for the history matching period ending at day 1286. Thereafter, and until day 2193, the simulation was run without re-matching the Ktzi 201 downhole pressure (see Fig. 2) exhibiting a continuation of the good matching results until the end of injection. From our point of view, the stop of injection operation for about seven months from day 1424 until day 1660 is an important indicator by means of model predictability, since reservoir pressure relaxation influences CO<sub>2</sub> volume expansion in the entire reservoir at the given time. An excellent downhole pressure match with insignificant deviations (< 0.05 %) was achieved for that period of operation emphasizing the reliability of the model in terms of reservoir pressure development prediction. From day 1680 on, CO<sub>2</sub> injection at the Ketzin pilot site was carried out by decreasing the injection temperature by 5 K per week instead of continuing injection at reservoir temperature to investigate the impact of cold injection on reservoir pressure and near-well temperature development. Independent of the fact that expansion of colder CO<sub>2</sub> implies an insignificant pressure increase due to the limited temperature difference, Ktzi 201 downhole pressure simulated with the isothermal ECLIPSE 100 simulator is about 1 % above the observed one, whereas the deviation decreases until the next injection stop at 1764 days. The following stop of

injection until day 1793 is again simulated with an excellent agreement between simulated and observed Ktzi 201 downhole pressure (deviation < 0.3 %). Changes in the EOS applied for density and viscosity calculation [22] as well as the required revision of near-well permeability tensors in the present ECLIPSE 100 model had a significant impact on the simulated CO<sub>2</sub> arrival times. Tab. 3 gives the resulting arrival times of dissolved and gaseous CO<sub>2</sub>, comparing the results to those presented by Kempka et al. [20]. While the deviation of the arrival time at the Ktzi 200 well increased by factor two to 12.9 %, the deviation of the arrival time at the Ktzi 202 well is remarkably small with 0.4 % following the undertaken model revision.

#### 4.2. Results from Approach II

##### *Inverse modeling for the first 50 days of injection*

Eleven time steps between 17 and 50 days (no data earlier than 17 days available) are used to fit the pressure for the first 50 days of injection. For the CO<sub>2</sub> arrival in Ktzi 200, a step function is applied for the inverse modelling (0 at the beginning and 1 when the CO<sub>2</sub> has arrived). Different combinations of estimated parameters were chosen with different weights given to the measurements. Below we present and discuss three of these cases.

Cases 1 and 2 apply an overall multiplier for permeability ( $M_K$ ) and porosity ( $M_{phi}$ ). In addition, the parameter  $n$  of the relative permeability for CO<sub>2</sub> (Eq. 1) is varied. The standard deviation for the arrival time is set to 0.02 and for the pressure to 10<sup>4</sup> Pa. The lower bound  $M_{phi}$  is decreased in Case 2 compared to Case 1 (0.6 instead of 0.7) with different starting values applied. Case 3 uses a different set of multipliers. The porosity field is still matched by adapting  $M_{phi}$ , whereas  $M_K$  depends directly on  $M_{phi}$  via the Kozeny-Carman [27] relation with a porosity of 0.2 as a basis:  $M_K = (M_{phi} \cdot 0.2)^3 \cdot (1 - 0.2)^2 / (0.2^3 \cdot (1 - M_{phi} \cdot 0.2)^2)$ . The lower limit for  $M_{phi}$  is set to 0.2. Further, the relative permeabilities for CO<sub>2</sub> ( $n_{CO_2}$ ) and water ( $n_w$ ) are varied separately. The standard deviation for the arrival time is increased to 0.05 to put more emphasis on the pressure fit.

The results of the three inversions are shown in Tab. 4. Fig. 2a compares the obtained pressure curves to the measurements for the first 50 days and shows a satisfactory match in all cases. The arrival times are matched much better by Cases 2 and 3. In Case 2, the relative permeability is the most sensitive parameter for the total matching in this particular case. It is most sensitive for the pressure, whereas porosity is the most sensitive for the arrival time. But one should keep in mind that sensitivities in the inversions strongly depend on the initial weighting of the measurements. Overall, the sensitivities of relative permeability, intrinsic permeability, and porosity for a best-fit to the monitoring data of the first 50 days of CO<sub>2</sub> injection are of comparable order of magnitude. Case 3 produces similar results as Case 2. The estimated parameter  $n_w$  represents an adjustment of the relative permeability curve and has only a small influence on the system behavior during the first 50 days. This is confirmed by the total sensitivity coefficients which are 218.4 for  $M_{phi}$  (including  $M_K$ ), 34.3 for  $n_{CO_2}$ , and only 10.8 for  $n_w$ . Thus, the variation of the porosity combined with permeability variation dominates the overall sensitivity of the system.

Table 4. Best-fit parameter sets from the inversion and corresponding arrival times of CO<sub>2</sub> at observation wells Ktzi 200 and Ktzi 202.

Case	Parameter 1	Parameter 2	Parameter 3	Arrival at Ktzi 200	Arrival at Ktzi 202
1	$M_K = 0.1067$	$M_\phi = 0.7048$	$n_{CO_2} = 1.5376$	24.98 days	317.47 days
2	$M_K = 0.1226$	$M_\phi = 0.6$	$n_{CO_2} = 1.1497$	21.71 days	216.60 days
3	$M_\phi = 0.5555, M_K = 0.1388$	$n_w = 9.46$	$n_{CO_2} = 1.3403$	21.81 days	210.16 days

##### *Testing the predictive capability: The time between 50 days and 1286 days*

The calibrated models (as discussed above) were then applied to simulate a longer time-scale. The pressure curves are presented in Fig. 2b for a period of 500 days. All the cases show deviations from the measured pressures. Case 1 starts diverging after about 180 days, Case 3 even earlier, while Case 2 matches the pressure well for about 380 days. In Case 1, both permeability ( $M_K=0.1067$ ) and relative permeability ( $n_{CO_2}=1.5376$ ) are lower compared to Case 2, probably the reason for the earlier increase of the pressure. The relative permeability of water seems to become more important after about 150 days when the CO<sub>2</sub> plume is bigger.

One should conclude that a perfect fit of the pressure curve over the whole simulation time with global multipliers for the entire domain is not possible without introducing more degrees of freedom than the three used in this exercise

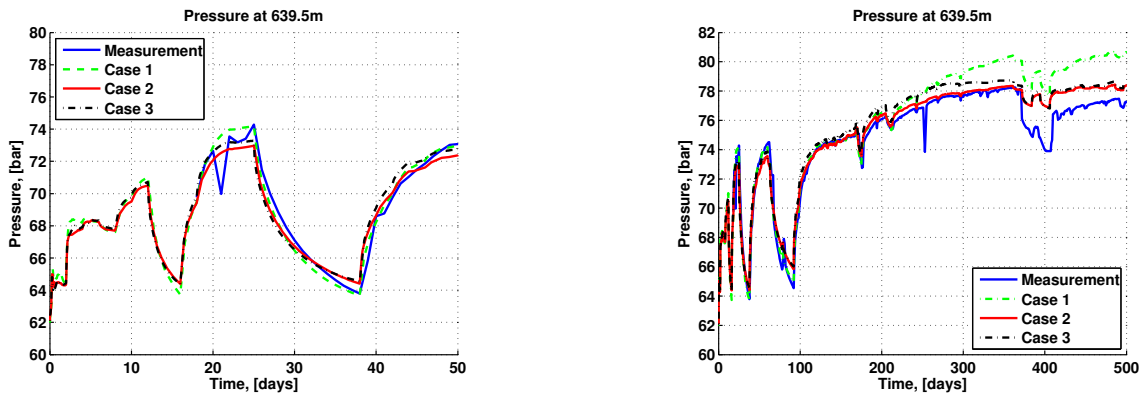


Fig. 2. Pressure evolution over time. a) For three different inversion cases at Ktzi 201. b) Extrapolation of the three cases to 500 days.

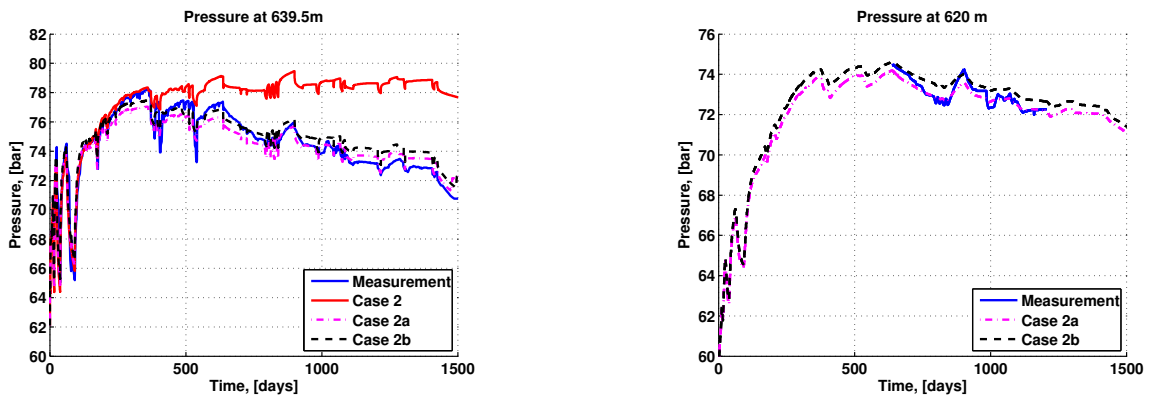


Fig. 3. Pressure evolution over time. a) For Case 2 and two far-field variations at Ktzi 201. b) For the two far-field variations of Case 2 at Ktzi 202.

up to here. Approach I [20] showed a better match by distinguishing between near-well and far-field multipliers for permeability. This distinction is adopted for Case 2 because it fits the pressure at least for 380 days and the most exact arrival time at the Ktzi 200 borehole is achieved. Within the far-field region, the original permeability and porosity values of the geological model are used. The multipliers of Case 2 for the porosity and the permeability are only applied in the near-well region. The relative permeability is the same in the whole domain ( $n_{CO_2}=1.1497$ ).

For Case 2a, a near-well region of  $1000\text{ m} \times 900\text{ m}$  is defined around the injection well (located at  $x=3242.7\text{ m}$  and  $y=2803.7\text{ m}$ ). As presented in Fig. 3a, the pressure curve is closer to the measurements at longer time scales and the trend of pressure decrease after 400 days can be observed for Case 2a. Since the pressure is underestimated between 200 days and 800 days, a second trial-and-error run with the near-well region enlarged by 100 m in every direction is performed (Case 2b). The pressure curve is then closer to the measurements for about 800 days compared to Case 2a. At time scales larger than 800 days, Case 2a fits the pressure curve better than Case 2b. The pressure measurements at Ktzi 202, only available between about 600 days and 1200 days after injection starts, are matched well in both cases (see Fig. 3b) with the maximum deviation in the order of 1 bar.

The remaining task is the matching of the arrival time at the Ktzi 202 borehole. In Case 2, the  $CO_2$  arrives after 216.6 days. The distinction between near-well and far-field leads to an even earlier arrival (208.52 days in Case 2a). For the two cases that fit the pressure well (Case 2a and Case 2b), a barrier-like feature (150 m long, 20 m wide) between the wells Ktzi 201 and Ktzi 202 is included (Case 2a-b1 and 2b-b2). The depth of the barrier is 5 m in Case 2a-b1 and 6 m in Case D-2b-b2 from the top of the domain. The arrival times at Ktzi 200 and Ktzi 202 for the different cases are 21.12 days and 208.52 days (Case 2a-farfield1), 21.51 days and 254.28 days (Case 2a-farfield1-b1), and 21.45 days and 264.47 days (Case 2b-farfield2-b2).

The barrier retards the arrival time as expected and the observed arrival of 271 days is almost achieved. Fig. 4 shows a section through Ktzi 201 and Ktzi 202 for Cases 2 and D-2b-b2 after 255 days. The CO<sub>2</sub> has already arrived at Ktzi 202 in Case 2, whereas it is shortly before arrival in Case 2b-b2. It is retained at the barrier and flows underneath until enough CO<sub>2</sub> has accumulated. Despite the hints on the probability that these kind of features might exist in the reservoir, the choice of inserting a barrier is, of course, somewhat arbitrary.



Fig. 4. Dumux model: Section through Ktzi 201 and Ktzi 202: CO<sub>2</sub> plume expansion after 255 days for Cases 2 and 2b-b2. The barrier feature can be detected as a blue rectangular spot in the right upper region of the right-hand figure.

#### Further extrapolation of matched models to most recent data

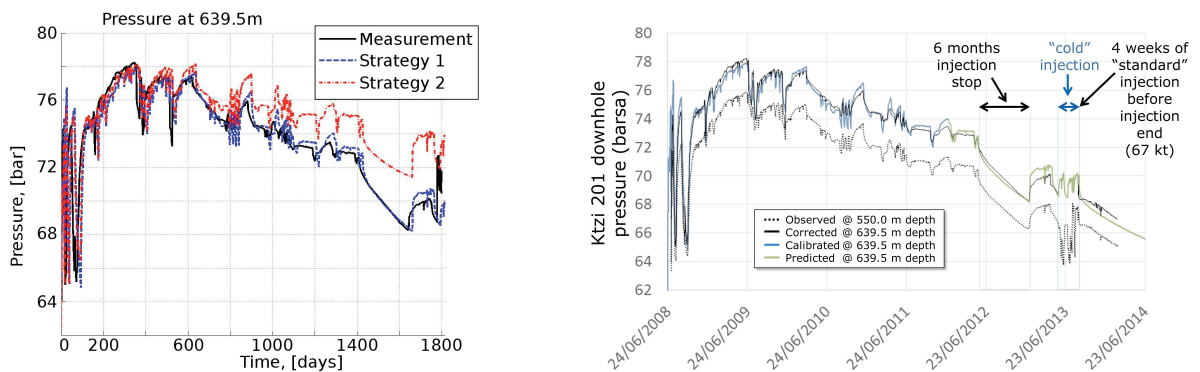


Fig. 5. Comparison of pressure in the injection well from measurement and from simulations: Left figure: Approach I (see Sec. 3.1) and II (Sec. 3.2). Right figure: Details of Approach I

The comparison between measurements and simulation for the full time period is shown in Fig. 5 (left). The Dumux model overestimates pressure at later times, while the amplitudes during shut-down and restart phases are still reproduced well. The Eclipse model (Approach I) matches the pressure response with excellent agreement, and the question turns up how this can be explained. For both approaches, the calibration is based on adapting the permeability. Dumux uses an anisotropy, which reduces the vertical permeability by a factor of 3. Thus, there is a tendency towards more horizontal flow in the modification according to Approach I (see Tab. 2), leading to a relatively stronger vertical CO<sub>2</sub> movement in Approach II, where more CO<sub>2</sub> spreads right underneath the top, then encountering regions of lower permeability and, thus, the pressure level is higher to push it forth. Hence, this realization of the geology as obtained from the modifications by Approach II seems to provide no satisfactory calibration at later times. Part of the deviations in Approach II, even though not quantifiable, are also due to a geological offset of about 10 m to 20 m in the far-field in the domain.

While discussing up to now mainly the differences in pressure responses, Fig. 6 gives an impression of the differences in CO<sub>2</sub> plume evolution. The top views of the plumes at different times are visibly different. However, since the details of the permeability field are associated with large uncertainties, it cannot be expected that a perfect match can be achieved, the more so as there is no further evidence than the arrival times in the observation wells.





Fig. 6. Permeability field (log scale) and CO<sub>2</sub> plume for mid of October 2009 (dark red) and 2012 (light red); Approach I left, Approach II right.

### 4.3. Conclusions

The results as presented above are obtained from work accompanying the Ketzin pilot project and were assembled for this study to summarize a number of interesting lessons that can be learned from the modeling work. First of all, we want to emphasize that the measurements and observations from the Ketzin project are well-controlled according to what the state-of-the-art allows. The Ketzin storage project is still far from the industrial scale. Thus, it should be expected that monitoring data from any present or future storage project is hardly available with higher reliability or accuracy. We should evaluate the results of this study in the light of this.

In general, it is costly and difficult to collect sufficient data from large-scale subsurface projects that allow predictive simulations. Data are of different accuracy, often only point-wise from boreholes. Thus, the required parameters for full-scale numerical models are associated with uncertainties. In order to make decisions based on numerical models it is usually required to quantify the uncertainties from data and models. This study does not cover the topic of uncertainties, but rather gives insights in data quality of actual projects and the range of interpretations with different models and different approaches. We can state at the end of this modeling exercise the following:

- Numerical simulation models were calibrated to available pressure data and observed arrival times.
- Parameters in the multiphase flow models are in parts strongly correlated to each other regarding their physical meaning. For example, relative permeabilities and intrinsic permeabilities have a high degree of correlation and are, thus, difficult to determine. The variation of porosity combined with permeability variation proved to be dominating the overall sensitivity of the simulated pressure values.
- The exact spatial distribution of permeabilities and porosities is currently impossible to determine. However, the basic response of the reservoir in terms of pressure increase due to injection of CO<sub>2</sub> can be calibrated and allows predictive simulations for pressure responses for a considerable time period. The variation of porosity combined with permeability variation proved to be dominating the overall sensitivity of the pressure responses.
- The matching of arrival times in strongly heterogeneous reservoirs is possible, while reliable long-term predictions of CO<sub>2</sub> plume evolution are more difficult to achieve. They strongly depend on geologic information and iterative integration of measurement data during the storage project.
- Quantification of uncertainties is a major task for future projects. This is computationally expensive and, for large-scale scenarios, requires sophisticated methods of model simplification, e.g. response surface methods.

*Acknowledgments:* The authors gratefully acknowledge the funding for the Ketzin project received from the European Commission (6th and 7th Framework Program), two German ministries - the Federal Ministry of Economics and Technology and the Federal Ministry of Education and Research - and industry since 2004. The ongoing R&D activities are funded within the project COMPLETE by the Federal Ministry of Education and Research. Further funding is received by VGS, RWE, Vattenfall, Statoil, OMV and the Norwegian CLIMIT programme.

## References

- [1] S. Martens, T. Kempka, A. Liebscher, S. Lüth, F. Möller, A. Myrntinen, B. Norden, C. Schmidt-Hattenberger, M. Zimmer, M. Kühn, Europe's longest-operating on-shore CO<sub>2</sub> storage site at Ketzin, Germany: a progress report after three years of injection, *Environmental Earth Sciences* 67 (2012) 323–334.
- [2] A. Förster, B. Norden, K. Zinck-Jorgensen, P. Frykman, J. Kulenkampff, E. Spangenberg, J. Erzinger, M. Zimmer, J. Kopp, G. Borm, C. Juhlin, C.-G. Cosma, S. Hurter, Baseline characterization of the CO<sub>2</sub>SINK geological storage site at Ketzin, Germany, *Environmental Geosciences* 13 (2006) 145–161.
- [3] C. Juhlin, R. Giese, K. Zinck-Jorgensen, C. Cosma, H. Kazemini, N. Juhojuntti, S. Lüth, B. Norden, A. Förster, 3D baseline seismics at Ketzin, Germany: the CO<sub>2</sub>SINK project, *Geophysics* 72 (2007) 121–132.
- [4] B. Norden, A. Förster, D. Vu-Hoang, F. Marcellis, N. Springer, I. Le Nir, Lithological and petrophysical core-log interpretation in CO<sub>2</sub>SINK, the European CO<sub>2</sub> onshore research storage and verification project., *SPE Reservoir Evaluation & Engineering* 13 (2) (2010) 179–192.
- [5] B. Wiese, B. J., C. Enachescu, H. Würdemann, G. Zimmermann, Hydraulic characterisation of the Stuttgart formation at the pilot test site for CO<sub>2</sub> storage, Ketzin, Germany, *International Journal of Greenhouse Gas Control* 4 (2010) 960–971.
- [6] E. Makhlof, M. Chen, W. Wasserman, J. Seinfeld, A general history matching algorithm for three-phase, three-dimensional petroleum reservoirs, *SPE Adv. Technol.* 1(2) (1993) 83–91.
- [7] M. Williams, J. Keating, M. Barghouty, The stratigraphic method: a structured approach to history-matching complex simulation models, *SPE Reserv.Evalu.Eng.* 1(2) (1998) 169–176.
- [8] S. Oladyskhin, H. Class, W. Nowak, Bayesian updating via bootstrap filtering combined with data-driven polynomial chaos expansions: methodology and application to history matching for carbon dioxide storage in geological formations, *Computational Geosciences* 17 (2013) 671–687.
- [9] Schlumberger, Eclipse reservoir engineering software version 2009.2 (2009).
- [10] B. Flemisch, M. Darcis, K. Erbertseder, B. Faigle, A. Lauser, K. Mosthaf, S. Müthing, P. Nuske, A. Tatomir, M. Wolff, R. Helmig, DuMu<sup>4</sup>: DUNE for multi-phase, component, scale, physics, ... flow and transport in porous media, *Advances in Water Resources* 34 (9) (2011) 1102–1112. doi:DOI: 10.1016/j.advwatres.2011.03.007.
- [11] H. Class, A. Ebigbo, R. Helmig, H. Dahle, J. Nordbotten, M. Celia, P. Audigane, M. Darcis, J. Ennis-King, F. Yaqing, B. Flemisch, S. Gasda, M. Jin, S. Krug, D. Lagregere, A. Naderi, R. Pawar, A. Sbai, S. Thomas, L. Trenty, L. Wei, A benchmark-study on problems related to CO<sub>2</sub> storage in geologic formations - summary and discussion of the results, *Computational Geosciences* 13 (2009) 409–434.
- [12] A. Förster, R. Schöner, H.-J. Förster, B. Norden, A.-W. Blaschke, J. Luckert, G. Beutler, R. Gaupp, D. Rhede, eservoir characterization of a CO<sub>2</sub> storage aquifer: The Upper Triassic Stuttgart Formation in the Northeast German Basin, *Marine and Petroleum Geology* 27(10) (2010) 2156–2172.
- [13] B. Norden, P. Frykman, Geological modelling of the Triassic Stuttgart Formation at Ketzin, Germany, *International Journal of Greenhouse Gas Control* 19 (2013) 756–774.
- [14] T. Kempka, H. Class, U. Görke, B. Norden, O. Kolditz, M. Kühn, L. Walter, W. Wang, B. Zehner, A dynamic flow simulation code intercomparison based on the revised static model of the ketzin pilot side, *Energy Procedia* 40 (2013) 418–427.
- [15] P. Bastian, M. Blatt, A. Dedner, C. Engwer, R. Klöforn, R. Kornhuber, M. Ohlberger, O. Sander, A generic grid interface for adaptive and parallel scientific computing., *Computing* 82 (2008) 103–119.
- [16] B. Prevedel, L. Wohlgemuth, B. Legarth, J. Henninges, H. Schütt, C. Schmitt-Hattenberger, et al., The CO<sub>2</sub>SINK boreholes for geological CO<sub>2</sub> storage testing, *Energy Procedia* 1 (2009) 2087–2094.
- [17] M. Zimmer, J. Erzinger, C. Kujawa, C. Group, The gas membrane sensor (GMS): A new method for gas measurements in deep boreholes applied at the CO<sub>2</sub>SINK site, *Intl. Journal of Greenhouse Gas Control* 5 (2011) 995–1001.
- [18] F. Schilling, G. Borm, H. Würdemann, F. Möller, M. Kühn, C. Group, Status Report on the First European on-shore CO<sub>2</sub> Storage Site at Ketzin (Germany), *Energy Procedia* 1 (2009) 2029–2035.
- [19] H. Würdemann, F. Möller, M. Kühn, W. Heidug, N. Christensen, G. Borm, F. Schilling, the CO<sub>2</sub>SINK Group, CO<sub>2</sub>SINK from site characterisation and risk assessment to monitoring and verification: One year of operational experience with the field laboratory for CO<sub>2</sub> storage at Ketzin, *International Journal of Greenhouse Gas Control* 4(6) (2010) 938–951.
- [20] T. Kempka, M. Kühn, Numerical simulations of CO<sub>2</sub> arrival times and reservoir pressure coincide with observations from the Ketzin pilot site, Germany., *Environmental Earth Sciences Special Issue* (2013) 1–11. doi:10.1007/s12665-013-2614-6.
- [21] T. Kempka, M. Kühn, H. Class, P. Frykman, A. Kopp, C. Nielsen, P. Probst, Modelling of CO<sub>2</sub> arrival time at Ketzin - Part I, *International Journal of Greenhouse Gas Control* 4 (2010) 1007–1015.
- [22] R. Span, W. Wagner, A New Equation of State for Carbon Dioxide Covering the Fluid Region from the Triple-Point Temperature to 1100 K at Pressures up to 800 MPa, *J. Phys. Chem. Ref. Data* 25(6) (1996) 1509–1596.
- [23] A. Peneloux, E. Rauzy, R. Freze, A consistent correction for RedlichKwongSoave volumes, *Fluid Phase Equilib.* 8 (1982) 7–23.
- [24] S. Finsterle, iTOUGH2 Sample Problems, Tech. rep., Lawrence Berkely National Laboratory, University of California (1999).
- [25] S. Martens, A. Liebscher, F. Möller, J. Henninges, T. Kempka, S. Lüth, B. Norden, B. Prevedel, A. Szizyalski, M. Zimmer, M. Kühn, CO<sub>2</sub> storage at the ketzin pilot site, germany: Fourth year of injection, monitoring, modelling and verification., *Energy Procedia* 37 (2013) 6434–6443.
- [26] F. Möller, A. Liebscher, S. Martens, C. Schmidt-Hattenberger, M. Kühn, Yearly operational datasets of the CO<sub>2</sub> storage pilot site ketzin, germany., Tech. rep., Geoforschungszentrum Potsdam, Scientific technical report: data 12/06 (pii0.2312/GFZ.b103-12066, online only) (2012).
- [27] A. Scheidegger, *The physics of flow through porous media*, Macmillian Co., New York, U.S.A., 1960.